Electronic Supplementary Material (ESI) for Journal of Materials Chemistry A

Nanoporous carbon synthesised with coal tar pitch and its capacitive performance

Liqun Wang, Jiuzhou Wang, Fan Jia, Chengyang Wang, Mingming Chen*

Table of Contents

* Key Laboratory for Green Chemical Technology of Ministry of Education, School of Chemical Engineering and Technology, Tianjin University, Tianjin, P. R. China. Email: chmm@tju.edu.cn (MM Chen)

Tel: +86 22-27890481; Fax: +86 22-27890481.

1. Synthesis of CP-A5 and CP-R5

The CP was pulverized to particles of 50-100 μm. Water-disperable part CP-A5 was synthesized by oxidation of CP powder with a mixture of concentrated nitric acid and sulfuric acid (v/v=3/7). The ratio of CP to oxidant is 1g: 5ml. After the reaction, the suspension was poured into cold water and adjusted pH to 7. The suspension was then filtrated. The residaul was washed with ionized water and dried, the product was marked as CP-R5. Dillute HCl was added into the filtrate untill the pH<2, a kind of precipitation was obtained, through washshing using dillute HCl and drying , we got a fine powder which was named as CP-A5.

2. Frequency analysis of the TEM image

Two-dimensional fast Fourier transform (FFT) of TEM image (fig.4a) was conducted, and the result is shown in the FFT power spectra of fig.4b. Masking step and inverse fast Fourier transform (IFFT) were taken place on the power spectrum to analyse the pores in more detail, fig. 4(c) and fig. 2(f). The specific frequency regions in reciprocal space were chosen by ring-shaped mask patterns, fig. 4(d) and fig. 4(g). The real space images were then transformed to binary pictures to observe the pore shapes more clearly, fig. 4(e) and fig. 4(h).

3. Tyndall effect of CP-A5 water dispersion

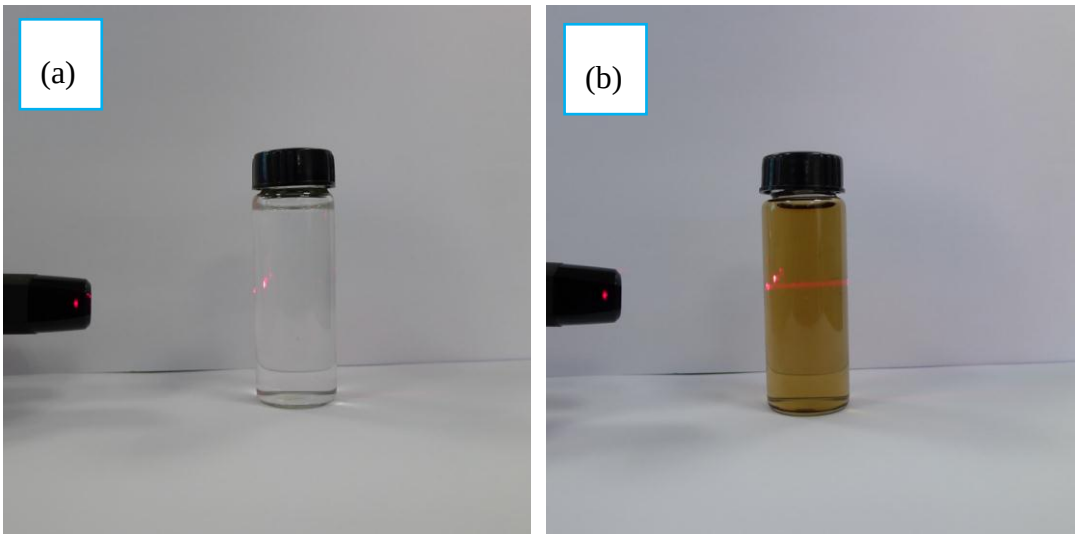

Fig. S1 (a) deionized water under irradiation of red laser; (b) 20mg L^{-1} intermediate CP-A5 dispered in deionized water and the light path of red laser.

4. FESEM image of the residual part CP-R5

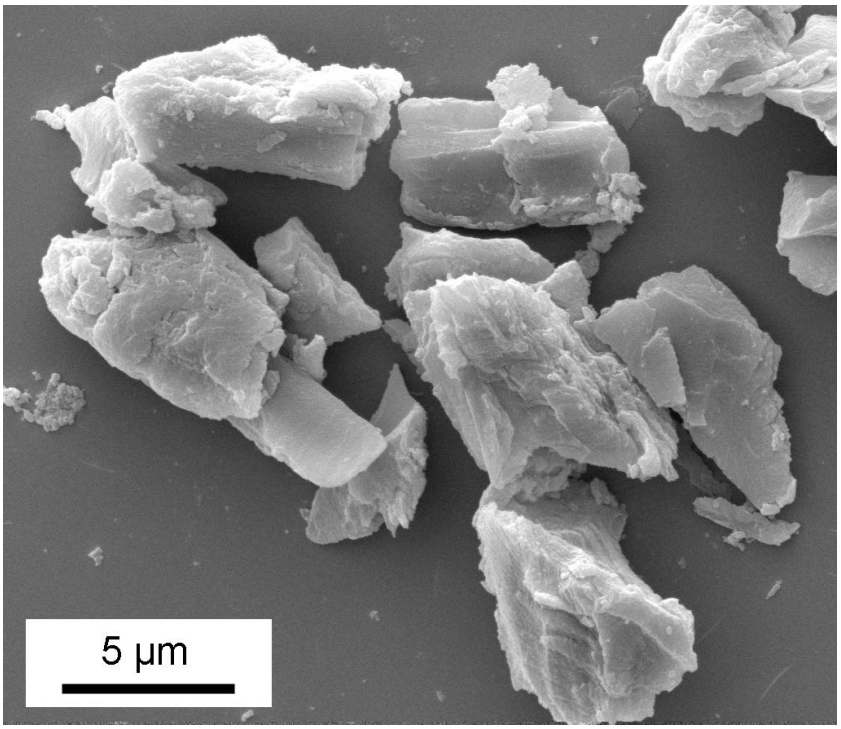

Fig. S2 FESEM image of the residual part CP-R5

5. C1s XPS high-resolution spectra of CP and CP-A5

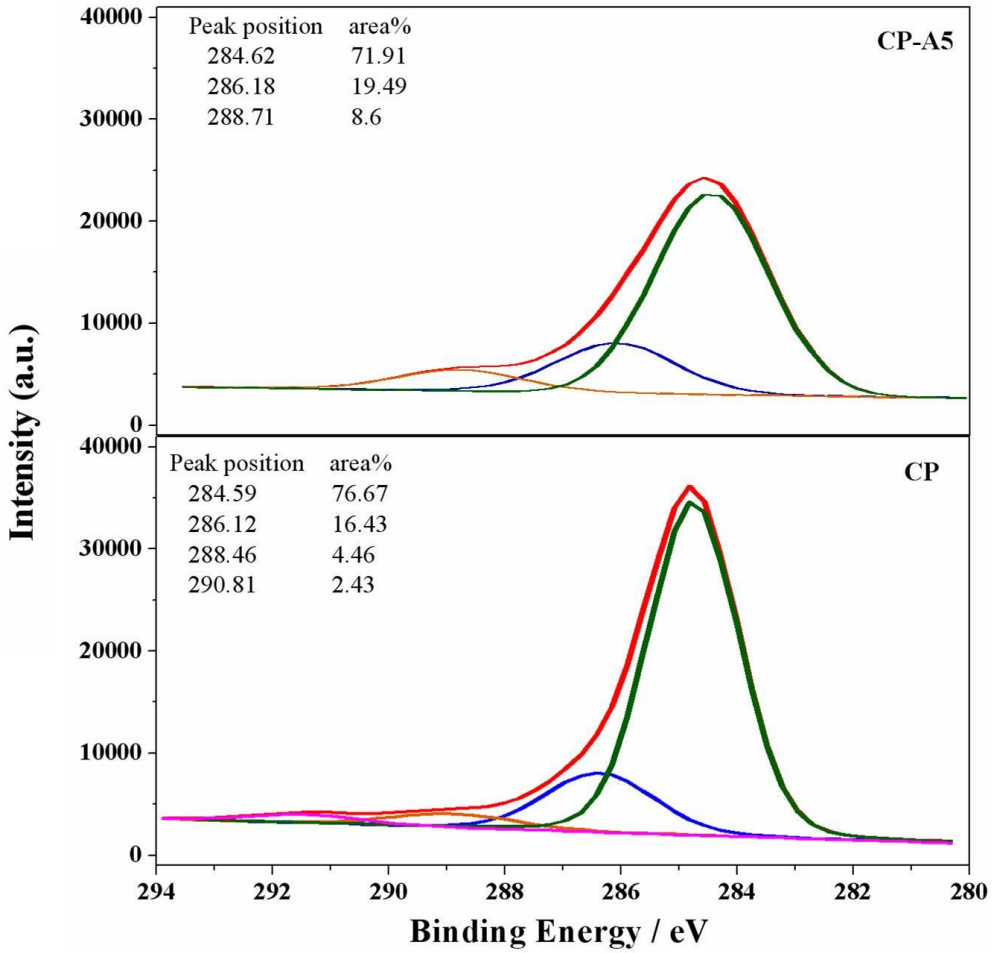

Fig. S3 C1s XPS high-resolution spectra of (a) CP-A5, and (b) CP

6. Electrochemical properties of CP-A5-3 and CP-A5-1.5

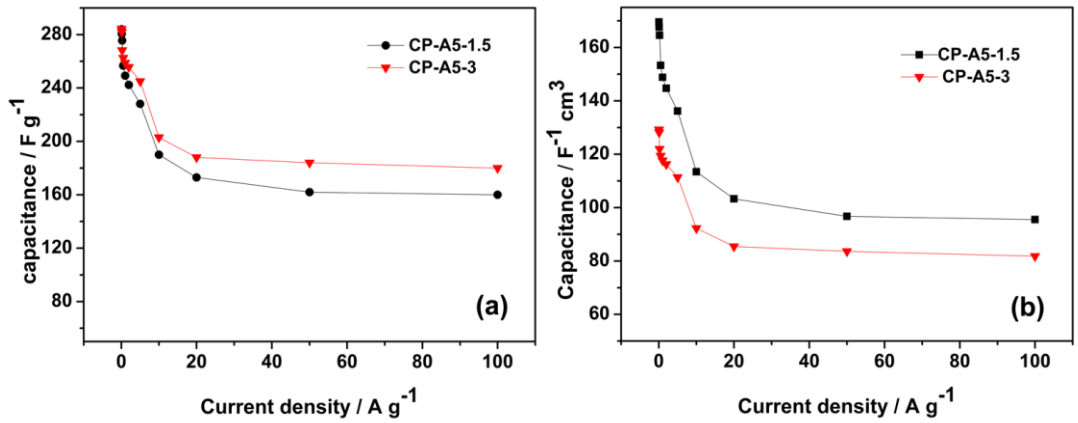

Fig. S4 Electrochemical properties of CP-A5-3 and CP-A5-1.5 in 6 M KOH solution: (a) gravimetric capacitances of single electrodes versus discharge current densities, (b) volumetric capacitances of single electrodes versus discharge current densities

7. Characterization of precursor $MnCO_3$ and hollow MnO_2

The synthesized $MnCO_3$ is cubic crystal (seen XRD pattern in fig. S5e, matching JCPDS card No.44-1472) and shows regular monodisperse cube-like morphology (fig. S5a) with the sizes from 100nm to 400nm. After the $KMnO_4$ oxidation, it chemically changes to gamma MnO_2 of poor crystalline (seen XRD pattern in fig. S5e, matching JCPDS card No.14-0644). Gamma MnO_2 (Fig. S5b) preserves the cube-like morphology of $MnCO_3$ precursor and the particle sizes are less than 400nm. Besides, the cavity could be clearly seen in fig. S5c and S5d，indicating the existence of hollow structure. The average shell thickness is about 27 nm. Based on the N_2 adsorption and desorption isotherms (fig. S5f), BET surface areas of the hollow MnO_2 were calculated to be 207 m^2 g^{-1}. X-ray photoelectron spectroscopic test (fig. S6) was conducted to evaluate the oxidation state of Mn in the surface of MnO_2 microcubes. The binding energies of Mn($2p^{3/2}$) and Mn($2p^{1/2}$) are 642.1 and 653.5 ev, respectively, which are well in accordance with MnO_2 [Mn($2p^{3/2}$) = 642.1 ev and Mn($2p^{1/2}$) = 653.8 ev] (J. Chastain, Handbook of X-ray Photoelectron Spectroscopy, 2nd ed., Perkin–Elmer Corporation, Wellesley, MA, 1992, 79.).

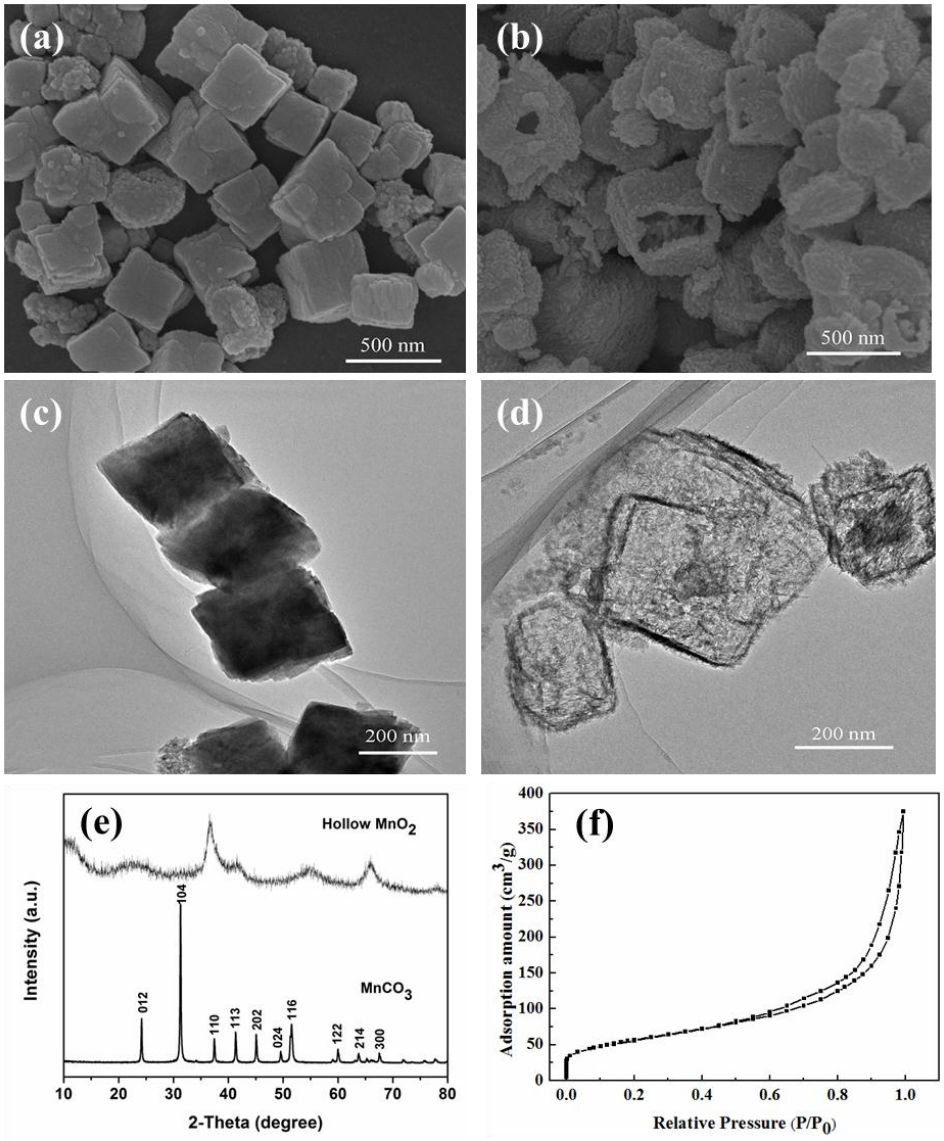

Fig. S5 Typical FESEM images and TEM images of the as-prepared product: (a, c) $MnCO_3$ precursor, (b, d) Hollow MnO_2 microcubes, (e) XRD patterns of $MnCO_3$ precursor and as prepared hollow MnO_2, (f) N_2 adsorption and desorption isotherms of hollow MnO_2 under 77K.

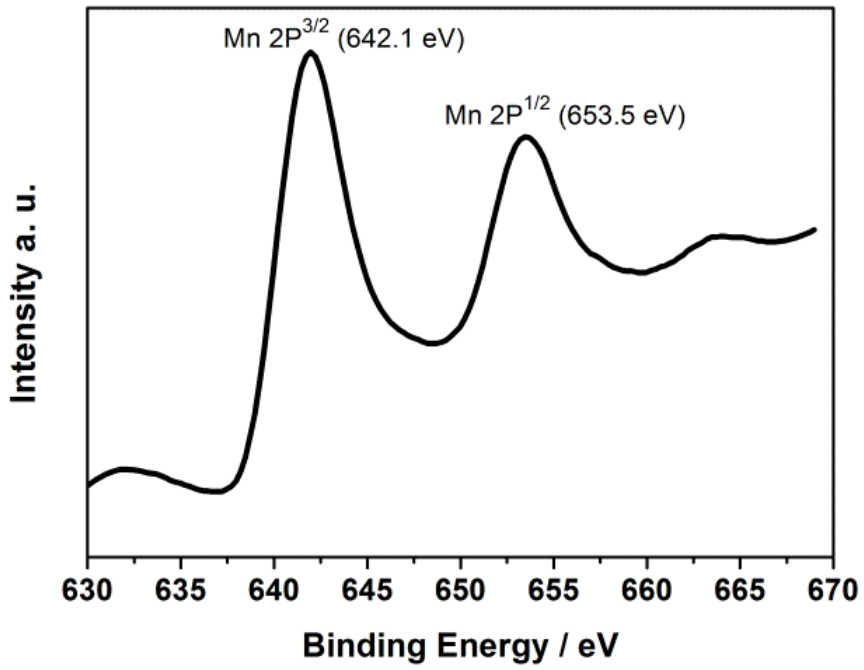

Fig. S6. XPS spectrum for Mn 2p core level of the hollow MnO_2 microcubes